

Optimal control of levitated nanoparticles through finite-stiffness confinement

Marco Baldovin,^{1,2,*} Ines Ben Yedder,³ Carlos A. Plata,⁴ Damien Raynal,^{3,5} Loïc Rondin,³ Emmanuel Trizac,^{2,6} and Antonio Prados⁴

¹*Institute for Complex Systems, CNR, Rome, I-00185 Italy*

²*Université Paris-Saclay, CNRS, LPTMS, Orsay, F-91405 France*

³*Université Paris-Saclay, ENS Paris-Saclay, CentraleSupélec, CNRS, LuMin, Orsay, F-91405 France*

⁴*Física Teórica, Universidad de Sevilla, Apartado de Correos 1065, Sevilla, E-41080 Spain*

⁵*Present address: Centre of Light for Life (CLL) and Institute for Photonics and Advanced Sensing (IPAS), The University of Adelaide, Adelaide, 5005, SA, Australia*

⁶*École Normale Supérieure de Lyon, Lyon, F-69342 France*

(Dated: August 2, 2024)

Optimal control of levitated particles subject to thermal fluctuations is a challenging problem, both from the theoretical and the experimental perspective. In this paper we compute the time-dependent harmonic confining potential that steers a Brownian particle between two assigned equilibrium states, in a prescribed time, with the minimum energetic cost. In our analysis we do not neglect inertial effects (thus addressing the general underdamped dynamics) and we assume, motivated by the experiments, that the stiffness of the confining potential cannot exceed prescribed bounds. We report the results of an experiment realizing the described protocol for an optically confined nanoparticle. The system is shown to reach the target state within accuracy, while spending less energy than other protocols that require the same time. The optimal protocol is also compared to an abrupt change of the confining stiffness, the latter involving an exponential relaxation to the target equilibrium state. Not only does our optimal protocol reach the target state in a finite time but it does so in a time significantly shorter than the characteristic timescale of the direct relaxation. The results presented in this paper are expected to have relevant applications in the design of optimal devices, e.g. engines at the nanoscale.

I. INTRODUCTION

The field of optimal control aims at devising time-dependent protocols for the parameters—stiffness of a harmonic trap, temperature of the heat bath, . . .—controlling the dynamical evolution of a system while minimizing a certain cost functional of its trajectory. This is relevant in a wealth of physical situations, although we focus here on the control of systems like nanodevices. Therein, we can highlight the minimization of entropy production [1–7] or the minimization of the connection time [8–12] between given initial and target states. Also, it has been shown that there emerge trade-off relations between the operation time and the cost, in terms of irreversible work or thermodynamic geometry quantities [13–17], which are known as the classical speed limits.

In principle, one could try to tackle the minimization problem of interest with the tools of calculus of variations, but this naive approach has several limitations; the main one stems from the impossibility of including restrictions on the protocols in the form of inequalities. This is not a formal, “mathematical”, problem but an essential one: in many experimental situations, the controlled parameters—control functions in the mathematical jargon—are restricted to a certain finite interval. Examples abound: the stiffness of a harmonic trap is typically limited to a certain range $\kappa_- \leq \kappa \leq \kappa_+$, depending

on the technique employed to realize the harmonic potential in the lab; the temperature of the heat bath may also be varied in a certain range $T_- \leq T \leq T_+$; in the former two cases, typically neither κ nor T can become negative.[18] The incorporation of these inequalities to the minimization problem entails the necessity of resorting to the more complex framework of Pontryagin’s Maximum Principle of optimal control theory [19], in order to find the optimal protocols.

Despite the advances in the control of colloidal particles during the last decade [20, 21], important aspects thereof still remain challenging. Notably, most of the theoretical [1, 3, 4, 6, 10, 12, 20, 22–25] and experimental results [26, 27] pertain to the overdamped regime, in which inertial effects are negligible. Therein, accelerating the connection between equilibrium states of a particle confined in an arbitrary potential has been shown to be feasible, by using inverse engineering techniques [22] and variants of the fast-forward [25] and the counterdiabatic [23] methods—imported from the field of shortcuts to adiabaticity developed in quantum mechanics [28]. Also, optimal protocols that make the connection and, in addition, minimize certain figure of merit have been investigated: for example, the minimization of the irreversible work—i.e., entropy production—for a given connection time t_f [1, 3, 4, 6]. In these works, the parameters characterizing the potential are assumed to be unbounded, and thus any two states can be connected and the connection time can be arbitrarily short—at the cost of an irreversible work diverging as t_f^{-1} . For the harmonic potential, the minimization of the irreversible work taking

* marco.baldovin@cnr.it

into account that the stiffness is bounded has also been investigated [24]: as a consequence, there appear states that cannot be reached and a minimum connection time for certain connections.

Extending such works to the underdamped situation is critical since it is the most general description and appears relevant from both an experimental and a theoretical perspective. From an experimental point of view, the underdamped regime emerges when considering nanomechanical resonators or levitated particles in moderate vacuum [29–33]. From a theoretical point of view, the problem is significantly more complex and less well understood than that of the overdamped regime. Inverse engineering techniques might be used, but there appear limitations—probably stemming from the hypotheses introduced to make analytical progress [34]. Optimal control of underdamped systems also brings about new challenges. On the one hand, optimal protocols in general involve non-conservative, velocity-dependent, drivings [5, 23, 35]. On the other hand, if one restricts oneself to position-dependent forces, as we do in the present paper, the optimal driving involves harsher discontinuities, of Dirac-delta type [2]. This is the consequence of the singular nature of the optimal problem, as it can be understood by studying regularized versions of the cost function [36]. In particular, the Dirac-delta discontinuity entails that these optimal protocols are not realizable in the lab since they involve infinite values of the harmonic stiffness.

The main goal of our paper is the optimal control of an underdamped particle, bringing to bear the practical limitations in the lab—bounded stiffness—in order to achieve the optimal realizable protocol. In particular, we aim at minimizing the irreversible contribution to the work—i.e., entropy production—for an underdamped particle that is confined in a harmonic potential, the elastic constant of which can be tuned at will in a certain interval $0 < \kappa_- \leq \kappa \leq \kappa_+$. Both the initial and target states are stationary, they are the equilibrium states corresponding to the initial and target values of the elastic constant. It is worth stressing that this is the only parameter that we control, i.e., the potential is harmonic, conservative, and confining for all times.

II. OPTIMAL CONTROL PROTOCOLS

Consider a Brownian particle of mass m , immersed in a fluid at constant temperature T , and let us denote by \mathbf{x} and \mathbf{v} its position and velocity. On the one hand, the thermal bath exerts on the particle a damping force $-\gamma\mathbf{v}$, where γ is a constant coefficient with the physical dimensions of mass over time. On the other hand, the random collisions with the fluid’s molecules result in a fluctuating force $\boldsymbol{\xi}(t)$ verifying

$$\langle \boldsymbol{\xi}(t) \rangle = 0, \quad (1a)$$

$$\langle \boldsymbol{\xi}(t)\boldsymbol{\xi}^T(t') \rangle = 2\gamma k_B T I \delta(t-t'), \quad (1b)$$

where I represents the identity matrix and k_B is the Boltzmann constant. If, along a certain direction, the particle is trapped by a confining harmonic potential with stiffness κ , the projection of the dynamics along that direction is

$$\dot{x} = v \quad (2a)$$

$$m\dot{v} = -\kappa x - \gamma v + \xi, \quad (2b)$$

which admits the equilibrium stationary state

$$p_{\text{eq}}(x, v|\kappa) = \frac{\sqrt{m\kappa}}{2\pi k_B T} \exp\left(-\frac{mv^2 + \kappa x^2}{2k_B T}\right). \quad (3)$$

The above notation emphasizes the fact that in typical experimental setups the confining potential’s stiffness κ is a controllable parameter, while T is usually fixed. We will assume that κ can be varied at will within the range

$$\kappa_- \leq \kappa \leq \kappa_+. \quad (4)$$

In many practical situations, it is required to quickly switch between an initial state $p_{\text{eq}}(x, v|\kappa_i)$ and a target equilibrium distribution $p_{\text{eq}}(x, v|\kappa_f)$ corresponding to different confinements. We ask

1. whether this task can be completed in a given finite time t_f , i.e., without waiting for the spontaneous relaxation of the system, by suitably steering κ within the range prescribed by (4);
2. what the protocol that minimizes, on average, the external work needed to complete the transition is.

In other words, we ask what time-dependent stiffness $\kappa(t)$ minimizes the quantity $\langle W(t_f) \rangle$, where

$$\langle W(t) \rangle = \int_0^t dt' \frac{\dot{\kappa}(t')}{2} \langle x^2(t') \rangle \quad (5)$$

is the cumulative work at time t .

By making use of Pontryagin’s theory for optimal control [19], in the “Materials and Methods” section we show that the answer to point 1 is positive whenever the total time t_f is larger than a certain threshold t_{th} depending on κ_i and κ_f . The latter is the minimum time needed to complete the transition via the 3-step “bang-bang” protocol

$$\kappa(t) = \begin{cases} \kappa_+ & 0, \leq t < t', \\ \kappa_-, & t' \leq t < t'', \\ \kappa_+ & t'', \leq t < t_{\text{th}}, \end{cases} \quad \text{if } \kappa_f > \kappa_i, \quad (6)$$

where t' and t'' are intermediate times, while $+$ and $-$ indices have to be switched if $\kappa_f > \kappa_i$. The threshold t_{th} can be computed with standard numerical methods: its dependence of t_{th} on κ_i and κ_f is also discussed in the “Materials and Methods” section. Strictly speaking, the condition $t_f \geq t_{\text{th}}$ is a *sufficient* condition: optimal solutions requiring times even smaller than t_{th} (involving

a larger number of bangs, i.e., constant- κ steps) might be possible in principle. However, we could not find any explicit example of those.

Regarding point 2, we show that the optimal connection, if t_f is sufficiently larger than t_{th} , is obtained as

$$\kappa(t) = \begin{cases} \kappa_+ & 0 \leq t < t_1, \\ \kappa_0(t), & t_1 \leq t < t_2, \\ \kappa_+, & t_2 \leq t < t_f, \end{cases} \quad \text{if } \kappa_f > \kappa_i, \quad (7)$$

where $\kappa_0(t)$, t_1 and t_2 are computed by (numerically) solving a system of ordinary differential equations, as detailed in the ‘‘Materials and Methods’’ section. For $\kappa_f < \kappa_i$, + and - subscripts have again to be switched. The system of differential equations in the intermediate interval, $t_1 \leq t < t_2$, is equivalent to that for the case of unbounded controls [2], but with different boundary conditions. Our discussion will mainly focus on protocols of the kind given in (7). If t_f is too close to t_{th} , more complex solutions are typically needed: we show some examples in the Supplemental Information.

III. EXPERIMENTAL RESULTS

To experimentally test the proposed optimal protocols, we use an optically levitated particle in moderate vacuum and at room temperature ($T_0 = 290$ K) [33]. An infrared laser is strongly focused by an objective to generate an optical tweezer that traps a 68 nm-radius spherical silica particle into a harmonic potential of natural frequency $\Omega \approx 2\pi \times 100$ kHz. The trap stiffness $\kappa = m\Omega^2$, with $m \approx 2.4 \times 10^{-18}$ kg the particle’s mass, is directly proportional to the trapping laser power P_{las} . The system damping is enforced via the gas pressure in the experiment chamber. We work at a gas pressure of $p_{gas} \approx 5$ hPa, corresponding to $\gamma/m = 2\pi \times 4.4$ kHz $\ll \Omega$, which allows us to work in the underdamped regime. Using an ancillary laser, we record the particle dynamics $x(t)$.

As discussed earlier, a critical limitation of experimental realizations of thermodynamics protocols is the access to a finite range of experimental parameters, which calls for bounded protocols. For instance, we control the trap stiffness through the trapping laser power using an acousto-optics modulator (AOM). This technically limits the range of available stiffness ratios to a factor of typically ten. We thus address decompression protocols with a compression factor $\chi = \kappa_f/\kappa_i = 0.5$, which are constrained by bounded stiffnesses between $\kappa_+ \approx 2.77$ pN/ μm ($\Omega_+ = 2\pi \times 170$ kHz) and $\kappa_- = 0.29$ pN/ μm ($\Omega_- = 2\pi \times 55$ kHz). In particular, we have picked $\kappa_i = \kappa_+$ and targetted a finite relaxation time t_f that we choose to be $\tau/3$ with $\tau = m/\gamma$ the natural relaxation time of the system. The associated optimal protocol, computed following the steps described in the previous section, is shown in red in the inset of Fig. 1.

We characterize the relaxation of the particle driven by this optimal protocol by studying its dynamics over

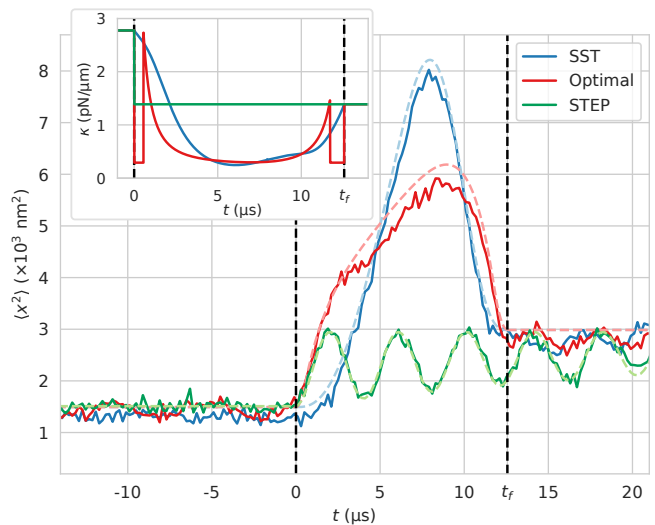


FIG. 1. Position variance of the particles over 30 000 realizations of a STEP (green), an SST (blue), and a bounded optimal (red) protocols. The associated stiffness are shown in the inset. The final time of SST and bounded optimal protocols is $t_f \approx 12.6$ μs . A fit of the STEP relaxation provides access to experimental parameters (red dashed line). The experimental variance evolutions associated with the SST and optimal protocols agree with analytical expectations (dashed lines). The vertical black dashed lines highlight the starting and final times of the protocols.

30 000 realizations of the protocol. As shown in red in Fig. 1, the resulting particle position variance $\langle x^2(t) \rangle$ reaches its steady-state equilibrium value at t_f and matches the theoretical expectation (dashed line). Thus, the designed bounded optimal protocols allow for reaching equilibrium at the targeted final time.

To assess the efficiency of this bounded optimal protocol in terms of work, we compare its realization with two other protocols with the same experimental constraints. First, a STEP protocol, corresponding to a sudden change of the stiffness from κ_i to κ_f (inset of Fig. 1, in green) and a swift state-to-state transformation (SST) that allows us to reach equilibrium in the finite time t_f [33, 34], shown in blue in the inset of Fig. 1.

As for the optimal bound protocols, we study the particle relaxation driven by these two protocols. The associated particle position variance is shown in Fig. 1. As expected, in the case of the STEP protocol, the variance presents oscillations with an exponential decay of characteristic time $\tau = m/\gamma \approx 3.8 \times 10^{-5}$ s, and it takes infinite time to reach exactly the target equilibrium state. Conversely, both the SST and the optimal protocols make it possible to reach the targeted final equilibrium state at the desired final time.

We then compute the mean experimental work required to drive the particle by the three protocols, using the definition given by (5). The computation is detailed in the ‘‘Material and Methods’’ section. The resulting experimentally measured cumulative work is dis-

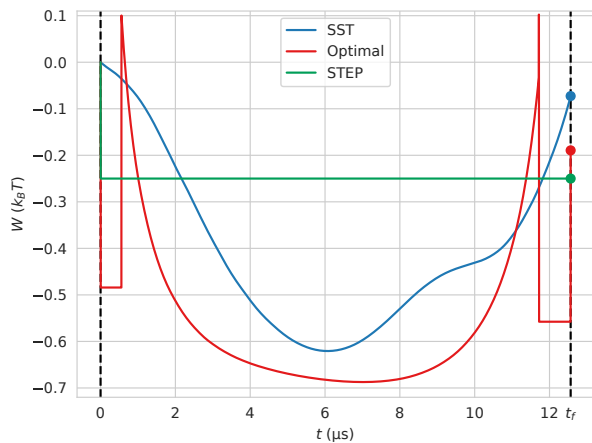


FIG. 2. Experimental cumulative work done for the STEP (green), SST (blue), and optimal bounded (red) protocols.

played in Fig. 2. At the protocols’ final time, we confirm that the bounded optimal protocol allows reaching equilibrium with work extraction corresponding to $W_{\text{optimal}} = -0.19 k_B T$ higher than in the case of the SST protocol under similar conditions ($W_{\text{SST}} = -0.07 k_B T$). The STEP protocol provides an even higher work extraction ($W_{\text{STEP}} = -\frac{k_B T}{4}$), but it must be noted that the system has not reached the target equilibrium state at t_f .

IV. DISCUSSION

The results shown in Figs. 1 and 2 account for a laboratory realization of the minimal-work transition between two equilibrium states of a levitated particle subject to thermal noise and viscous friction, in a regime where inertial effects are relevant. The control protocol for the confining potential detailed in the “Materials and Methods” section is applied within an actual experimental setup, showing that it can be implemented up to a very good degree of approximation. The target state is reached with the same accuracy as with the non-optimized SST protocol studied in [33], but with a somewhat lower energetic cost. The naive STEP protocol obtained by abruptly changing the confining stiffness and waiting for relaxation leads instead to a state which is far from being thermalized at the prescribed final time.

The present experiment puts forward a proof of principle for optimal control protocols at the nanoscale, by showing that fast optimized transitions are realizable in the lab with levitated particles. Moreover, the results reported here are expected to be relevant, for instance, for the realization of thermal engines at scales where thermal effects are not negligible and stochastic thermodynamics must be taken into account. Minimizing work done on the system—i.e., maximizing work extracted from it—at constant bath temperature is a typical building block in the design of efficient thermodynamic cycles:

e.g. this corresponds to the optimal isothermal branches of a maximum-power irreversible Carnot engine [37].

From the theoretical point of view, a challenging point to be further explored is the limit case of connection times close to the threshold established by the 3-step protocol: the minimal work is usually not given by a 3-stage process, and more complex behaviors need to be taken into account. Another possible research line concerns the more general case of non-harmonic confinements, theoretically discussed in [38, 39] in the limit of small inertial effects, without explicit bounds on the stiffness. Finally, an interesting field of investigation concerns the extension of control techniques to active-matter systems [40, 41], for which some theoretical results are already available [42, 43].

V. MATERIALS AND METHODS

In this section, we first provide the analytical derivation of (6) and (7), and numerical strategies to compute the corresponding optimal protocols. Then we enter into the details of the experimental setup.

A. Pontryagin’s approach

The main tool for the derivation of our analytical results is Pontryagin’s maximum principle [19, 44]. In a nutshell, this central result of control theory allows to find necessary conditions for the time-dependent protocol $k(t)$ that minimizes the cost

$$C = \int_0^{t_f} dt g[\mathbf{u}(t), k(t)] \quad (8)$$

along the evolution of a generic dynamical system

$$\dot{\mathbf{u}}(t) = \mathbf{f}[\mathbf{u}(t), k(t)] \quad (9)$$

in the time interval $0 \leq t \leq t_f$. The first step is to define the Hamiltonian

$$\mathcal{H}(\mathbf{u}, \boldsymbol{\varphi}, k) = \varphi_0 g(\mathbf{u}, k) + \boldsymbol{\varphi} \cdot \mathbf{f}(\mathbf{u}, k), \quad (10)$$

where $\boldsymbol{\varphi}$ is the vector of the conjugated momenta of \mathbf{u} , while $\varphi_0 \leq 0$ is a constant. The evolution of the system in this enlarged symplectic space is given by

$$\dot{\mathbf{u}} = \nabla_{\boldsymbol{\varphi}} \mathcal{H}, \quad \dot{\boldsymbol{\varphi}} = -\nabla_{\mathbf{u}} \mathcal{H}. \quad (11)$$

The minimization is then obtained by searching, at each time, for the value of k that maximizes \mathcal{H} :

$$k(t) = \arg \sup_k \mathcal{H}(\mathbf{u}, \boldsymbol{\varphi}, k).$$

This optimal $k(\mathbf{u}, \boldsymbol{\varphi})$, when inserted into the canonical equations, leads to an optimal trajectory $(\mathbf{u}(t), \boldsymbol{\varphi}(t))$ in phase space. The candidate thus obtained,

$\{k(t), \mathbf{u}(t), \varphi(t)\}$, must verify $(\varphi_0, \varphi) \neq (0, \mathbf{0})$ for all $t \in [0, t_f]$ to provide a solution for the minimization problem. Over the solution $\{k(t), \mathbf{u}(t), \varphi(t)\}$ found in this way, the Hamiltonian is constant, independent of time. We note that, when no bounds are present on k , the above strategy provides the usual Euler-Lagrange equations, with φ playing the role of the Lagrange multipliers ensuring that the dynamical system defined by (9) holds.

In order to exploit Pontryagin's principle, we need to reshape the Langevin equation (2) into the form of a dynamical system. The probability density function $p(x, v, t)$ of position and velocity evolves through the Klein-Kramers equation

$$\partial_t p = -\partial_x (vp) + \frac{1}{m} \partial_v \left(\kappa xp + \gamma vp + \frac{\gamma k_B T}{m} \partial_v p \right), \quad (12)$$

which is equivalent to (2) [45]. If the starting condition is a Gaussian distribution centered at $(x = 0, v = 0)$, as is the case at equilibrium, (12) ensures that this property is preserved during the whole evolution. The state of the system is then completely characterized by its second moments or, equivalently, by the vector \mathbf{u} with dimensionless elements:

$$u_1 = \frac{\gamma^2}{k_B T m} \langle x^2 \rangle, \quad u_2 = \frac{\gamma}{k_B T} \langle xv \rangle, \quad u_3 = \frac{m}{k_B T} \langle v^2 \rangle. \quad (13)$$

By also introducing the rescaled time s and stiffness k as

$$s = \frac{\gamma t}{m}, \quad k = \frac{m\kappa}{\gamma^2}, \quad (14)$$

the evolution of the system's state can be written as

$$\frac{d}{ds} \mathbf{u} = \mathbf{M}_k \mathbf{u} + 2\mathbf{e}_3 \quad (15)$$

with

$$\mathbf{M}_k = \begin{pmatrix} 0 & 2 & 0 \\ -k & -1 & 1 \\ 0 & -2k & -2 \end{pmatrix}, \quad \mathbf{e}_3 = \begin{pmatrix} 0 \\ 0 \\ 1 \end{pmatrix}. \quad (16)$$

B. Minimal time

We are now ready to make use of Pontryagin's principle. We want to connect the two equilibrium steady states with different stiffnesses k_i and k_f ,

$$\mathbf{u}_i = \begin{pmatrix} 1/k_i \\ 0 \\ 1 \end{pmatrix} \quad \text{and} \quad \mathbf{u}_f = \begin{pmatrix} 1/k_f \\ 0 \\ 1 \end{pmatrix}. \quad (17)$$

We allow $k(s)$ to vary with arbitrary speed, and even to make discontinuous jumps, but require it to remain within the bounds prescribed by (4), namely

$$\frac{m\kappa_-}{\gamma^2} = k_- \leq k \leq k_+ = \frac{m\kappa_+}{\gamma^2}. \quad (18)$$

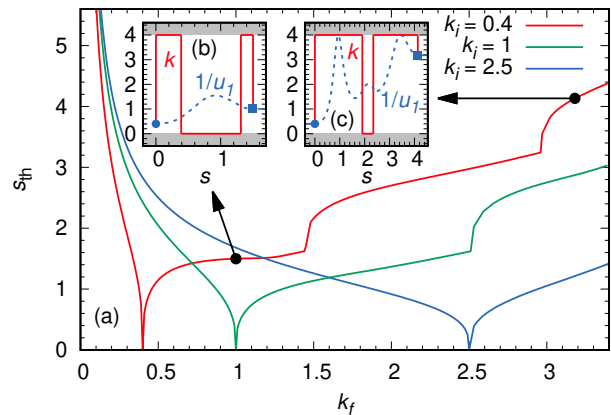


FIG. 3. Minimal time protocols. In the main panel (a) the dependence of the minimal connection time for a 3-step protocol (6) is shown as a function of the final (rescaled) stiffness k_f , for different values of k_i . Insets (b) and (c) show the explicit protocol k (red, solid) and the inverse of the rescaled position variance, $1/u_1$ (blue, dashed), for the two cases ($k_i = 0.4$, $k_f = 1$) and ($k_i = 0.4$, $k_f = 3.18$). Shaded areas correspond to values of the stiffness that are not allowed. Here $k_- = 0$ and $k_+ = 4$.

The first question we address is whether it is possible to design a time-dependent control protocol $k(s)$ that enforces this transition. Let us notice that, if a protocol $k^*(s)$ completes the task in a time s_f^* , the protocol

$$k(s) = \begin{cases} k^*(s), & 0 < s < s_f^*, \\ k_f, & s_f^* < s < s_f, \end{cases}$$

does the job for every time interval $s_f > s_f^*$. Indeed, after time s_f^* , the system just remains in the equilibrium state corresponding to $k = k_f$. The problem is then reduced to finding the minimum possible connection time s_{th} , given the boundary conditions \mathbf{u}_i and \mathbf{u}_f : if $s_f \geq s_{th}$, the transition can be surely completed.

In terms of Pontryagin's principle, we need to minimize the cost

$$C = s_{th} = \int_0^{s_{th}} ds,$$

leading to the Hamiltonian

$$\mathcal{H} = -\varphi_0 + \varphi \cdot (\mathbf{M}_k \mathbf{u} + 2\mathbf{e}_3). \quad (19)$$

We need to find, at each time, the value of k that maximizes \mathcal{H} . There are two possibilities: either k is a solution of

$$\frac{\partial \mathcal{H}}{\partial k} = 0, \quad (20)$$

or it coincides with one of the boundary values k_{\pm} . In the former case, condition (20) leads to the identity

$$\varphi_2 u_1 + 2\varphi_3 u_2 = 0. \quad (21)$$

Time-derivative yields, bearing in mind (11),

$$\varphi_2 \frac{\partial \mathcal{H}}{\partial u_1} - u_1 \frac{\partial \mathcal{H}}{\partial \varphi_2} + 2\varphi_3 \frac{\partial \mathcal{H}}{\partial u_2} - 2u_2 \frac{\partial \mathcal{H}}{\partial \varphi_3} = 0.$$

Hence, making use of (20),

$$\varphi_1 u_1 - \varphi_3 u_3 = 0. \quad (22)$$

Taking again time derivative, one obtains

$$2\varphi_1 u_2 + \varphi_2 u_3 - 2\varphi_3 = 0$$

which, once coupled with (21) and (22), only admits the trivial solution $\varphi_1 = \varphi_2 = \varphi_3 = 0$. In addition, for the time minimization problem, the Hamiltonian identically vanishes over the optimal trajectory. This entails that $\varphi_0 = 0$, and therefore this candidate cannot be a solution of the minimization problem. The above discussion implies that $\partial H / \partial k \neq 0$ over a finite time interval of the solution of the minimization problem. Therefore, depending on the sign of $\partial H / \partial k$, the optimal value of k would be either k_+ or k_- . The optimal protocol is therefore composed of intervals where $k = k_+$ and intervals where $k = k_-$ (“bang-bang” protocol [8, 9, 11, 12, 46–49]), with the “switchings” between these values taking place at the times for which $\partial H / \partial k = 0$. This kind of protocols often appear as solution candidates for minimal-time problems [8, 9, 11, 12, 49], although a rigorous proof that it is the solution of the minimum time problem is only available when the Hamiltonian is linear in both \mathbf{u} and the control—which is not the present case, since M_k depends on k .

The minimum number of switchings between k_+ and k_- that we need, in order to match the boundary conditions, can be computed in this way: of the six conditions provided by (17), three can be matched by the additive constants of the ordinary differential equations (15), while the remaining three need the introduction of an equal number of additional degrees of freedom (two switching times, s' and s'' , and the final time s_{th}). The switching times can be found by noticing that, for fixed values of $k = k_{\pm}$, the dynamics (15) is linear in the translated variables

$$\mathbf{u}_{\pm} = \mathbf{u} - \mathbf{r}_{\pm} \quad \text{with} \quad \mathbf{r}_{\pm} = \begin{pmatrix} 1/k_{\pm} \\ 0 \\ 1 \end{pmatrix}.$$

The final state corresponding to the protocol (6) for $\text{sgn}(k_f - k_i) = \pm 1$ can be then explicitly computed as a function of s' , s'' and s_{th} :

$$\mathbf{u}(s') = \mathbf{r}_{\pm} + \exp[s' M_{k_{\pm}}] (\mathbf{u}_i - \mathbf{r}_{\pm}), \quad (23a)$$

$$\mathbf{u}(s'') = \mathbf{r}_{\mp} + \exp[(s'' - s') M_{k_{\mp}}] (\mathbf{u}(s') - \mathbf{r}_{\mp}), \quad (23b)$$

$$\mathbf{u}(s_{\text{th}}) = \mathbf{r}_{\pm} + \exp[(s_{\text{th}} - s'') M_{k_{\pm}}] (\mathbf{u}(s'') - \mathbf{r}_{\pm}). \quad (23c)$$

By imposing $\mathbf{u}(s_{\text{th}}) = \mathbf{u}_f$, one has 3 equations to be solved for s' , s'' and s_{th} : the solution can be obtained

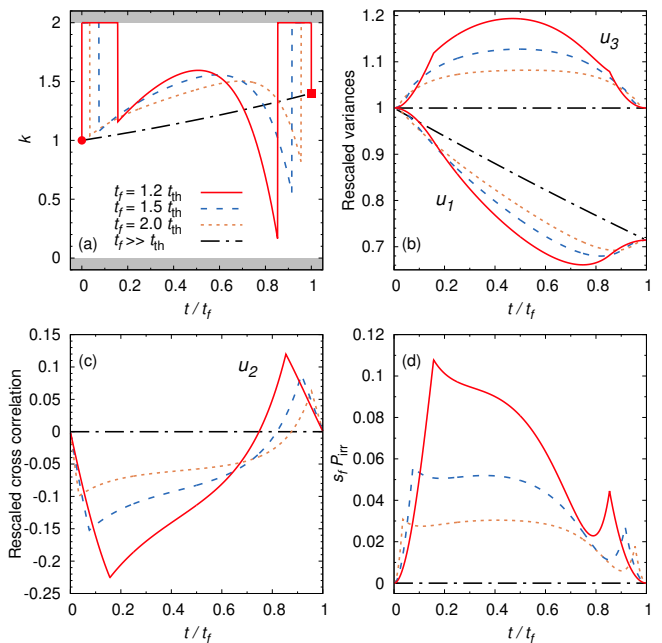


FIG. 4. Minimal work protocols. Panel (a) shows some examples of protocol (7), for different values of the connection time t_f . The dash-dotted black curve corresponds to the quasi-static limit, shaded areas denote forbidden values of the stiffness. In panels (b) and (c) the behavior of the rescaled moments u_1 , u_2 and u_3 is shown in the same conditions. Finally, panel (d) exhibits the time dependence of the irreversible part of the average power (the integrand in the r.h.s. of (24)). The plot axes are rescaled in such a way that the total area below each curve is proportional to the irreversible work done during each process: as expected, its value decreases when increasing t_f . Here $k_i = 1$, $k_f = 1.4$, $k_- = 0$, $k_+ = 2$.

numerically. The value of s_{th} found in this way is the threshold for the protocol to exist. Its dependence on the boundary conditions is explored numerically, for fixed k_- and k_+ , in Fig. 3.

Here, we have only considered 3-step protocols of the form (6), but solutions with a larger number of switchings are in principle possible. From a physical point of view, one expects the solution with the minimum number of switchings to provide the minimum connection time. In fact, this has been proved in other non-linear control problems [11, 49], although we do not have a rigorous proof for our case.

C. Minimal work

Once it has been established that a transition between given equilibrium states can be achieved in a time $s_f \geq s_{\text{th}}$, the next step is to search for the protocol that minimizes the total work. We show in the Supplemental Material that the total average work (5) can be split into two contributions: (i) a reversible one, which only depends on the boundary conditions and is physically re-

lated to the free energy variation; and (ii) an irreversible one

$$\langle W_{\text{irr}} \rangle = \int_0^{s_f} ds \left(\frac{u_1}{u_1 u_3 - u_2^2} + u_3 - 2 \right), \quad (24)$$

which intrinsically depends on the chosen protocol, and vanishes in the quasi-static limit (i.e., when the transition is achieved in a diverging time, as a sequence of equilibrium states). These findings are consistent with known results of stochastic thermodynamics [5]. The optimal solution can be found by minimizing either $\langle W_{\text{irr}} \rangle$ directly, or the cost function

$$C = \gamma \int_0^{t_f} dt \langle v^2 \rangle - \frac{\gamma}{m} k_B T t_f, \quad (25)$$

which in dimensionless units reads

$$C = \int_0^{s_f} ds (u_3 - 1). \quad (26)$$

As discussed in the Supporting Information, this cost function is the excess work with respect to the energy variation, and the two approaches are equivalent because the boundary conditions are fixed. Pontryagin's Hamiltonian for this problem reads then

$$\mathcal{H} = -u_3 + 1 + \boldsymbol{\varphi} \cdot (M_k \mathbf{u} + 2\mathbf{e}_3) \quad (27)$$

where $\boldsymbol{\varphi}$ is the vector of the moments conjugated to \mathbf{u} , normalized in such a way that the constant φ_0 is equal to -1.

Also in this case we start searching for stationary points satisfying (20). The condition reduces to

$$u_1 \varphi_2 + 2u_2 \varphi_3 = 0. \quad (28)$$

As we did before for the minimal time case, we consider the time derivative of the above identity, leading to

$$u_1 \dot{\varphi}_1 - \dot{u}_2 - u_3 \dot{\varphi}_3 = 0 \quad (29)$$

once the conditions (11) are taken into account. The time derivative of (29) implies

$$k u_1 + u_2 - 2u_3 + 2u_2 \dot{\varphi}_1 + u_3 \dot{\varphi}_2 - 2\dot{\varphi}_3 = 0. \quad (30)$$

At variance with the case considered before, now the three equations for $\boldsymbol{\varphi}$ do depend on k , and therefore they may admit a nontrivial solution. By taking the derivative with respect to s once again, making repeated use of (11) and taking into account Eqs. (28)-(29), one has finally

$$\frac{dk}{ds} = 3k + \frac{6}{u_1} + 3\frac{u_2}{u_1} - 9\frac{u_3}{u_1} + 10\frac{u_2^2}{u_1^2} - 8\frac{u_2 u_3}{u_1^2} + 8\frac{u_2^3}{u_1^3}. \quad (31)$$

Once coupled with the dynamics of \mathbf{u} (15), the above relation provides a 4-th order differential system, which is equivalent to the one found in [2]. Let us call $k_0(s)$

its solution, specified up to four degrees of freedom. It is important to note that the boundary conditions we enforce to determine k_0 are different from the ones considered in [2]: therein, the target state was not enforced to be the equilibrium state corresponding to the final value of the stiffness. In other words, the final state in the SST connection developed in [2] would evolve in time for times longer than t_f , whereas our system remains stationary for $t > t_f$. Note that the function $k_0(s)$ alone, with our boundary conditions, cannot be the solution of our problem—it does not have enough degrees of freedom to match the boundary conditions. Moreover, this difficulty cannot be solved by introducing Dirac-delta jumps at the initial and final times, because of the bounds in the stiffness in (4)—or (18). Reasoning as we did for the minimal-time case, and taking into account the fact that now the final time s_f is fixed, we realize that the simplest possible solution satisfying all the boundary conditions is obtained by alternating two intervals at fixed $k = k_{\pm}$ (from $s = 0$ to $s = s_1$ and from $s = s_2$ to $s = s_f$) with an interval (from s_1 to s_2) at $k = k_0(s)$. Examples are shown in Fig. 4. The optimal protocol (7) is recovered by turning back to dimensional variables, $\kappa(t) = \gamma^2 k(t)/m$.

Is it always possible to work out a solution of this sort? To answer this question, it is useful to notice that in the limit $s_f \rightarrow \infty$ we expect a time-scale separation between the (slow) dynamics of the control and the (fast) thermalization of the system. The optimal solution tends to coincide with its overdamped limit [5, 36], namely

$$k(s) = \left(\frac{s_f - s}{\sqrt{k_i s_f}} + \frac{s}{\sqrt{k_f s_f}} \right)^{-2}, \quad (32)$$

which can be realized without exceeding the range $k \in [k_i, k_f] \subset [k_-, k_+]$. We expect therefore the optimal solution in the time interval $[s_1, s_2]$, determined by $k_0(s)$, to stay in the range $[k_-, k_+]$ if $t_f \gg t_{\text{th}}$. If t_f is larger than t_{th} , but quite close to it, a more complex shape may be required. An explicit example is considered in the Supplemental Information.

D. Calibration of experimental trajectories time traces

The particle position $x(t)$ is experimentally measured using a photodetector. The recorded voltage writes

$$V_x(t) = c_x x(t) + N(t), \quad (33)$$

where c_x is the position calibration factor, and N is the experimental noise assumed to be uncorrelated with the particle displacement. Consequently, the variance of the measured signal writes

$$\sigma_V^2 = c_x^2 \sigma_x^2(t) + \sigma_N^2. \quad (34)$$

One can show that in the case of the STEP protocol,

the particle position variance is given by [33]

$$\sigma_x^2(t) = \sigma_i^2 \frac{\chi - 1}{2\chi} [1 + \cos(2\Omega_f t)] e^{-\gamma t} + \frac{\sigma_i^2}{\chi}. \quad (35)$$

Experimentally, we enforce the compression factor $\chi = 0.5$, the trap frequency Ω_f , i.e., κ_f , and the initial and final position variances through the equipartition theorem

$$\sigma_i^2 = \frac{k_B T}{\kappa_i}, \quad \sigma_f^2 = \frac{k_B T}{\kappa_f}. \quad (36)$$

Thus, from a fit of the experimental STEP protocols, we can retrieve the values of c_x and σ_N to determine the actual particle position variance.

E. Computation of the mean experimental work

The cumulative work up to time t is given by (5). For protocols without stiffness discontinuity (SST, or Euler-Lagrange part of the bounded optimal protocols), we can compute numerically the integral (5), where we use the theoretical value of κ and the experimentally measured value of σ_x . For protocols with stiffness discontinuity at time t_d , the associated instantaneous work is

$$\langle W_d(t_d) \rangle = \frac{1}{2} [\kappa(t_d^+) - \kappa(t_d^-)] \langle x^2(t_d^-) \rangle. \quad (37)$$

To minimize the impact of the exact choice of t_d^- on the computation, we oversample the experimental data to get a smaller time step ($\delta t_{W, \text{oversampled}} = 1.6$ ns, and $\delta t_{\text{acquisition}} = 200$ ns). We note that this oversampling

neither affects, beyond measurement uncertainties, the computation of the work on the Euler-Lagrange segment of the optimal protocols nor on the SST protocol.

In the case of the STEP protocols, since they have been used to calibrate our measurement scheme by construction, the associated work is given by

$$\langle W_{\text{STEP}} \rangle = \frac{1}{2} (\kappa_f - \kappa_i) \sigma_i^2 = \frac{k_B T}{2} (\chi - 1) = -\frac{k_B T}{4}, \quad (38)$$

for our choice $\chi = 0.5$.

Note that we assumed that the discontinuities are perfectly stiff, since the typical time required to change the stiffness is $\tau_{\text{raise}} \approx 200$ ns, much shorter than all other timescale of the problem.

ACKNOWLEDGMENTS

MB thankfully acknowledges useful discussions with J. Sanders and P. Muratore-Ginanneschi. MB was supported by ERC Advanced Grant RG.BIO (Contract No. 785932). CAP and AP acknowledge financial support from Grant PID2021-122588NB-I00 funded by MCIN/AEI/10.13039/501100011033/ and by ‘‘ERDF A way of making Europe’’. CAP, AP, and ET acknowledge financial support from Grant ProyExcel_00796 funded by Junta de Andaluc a’s PAIDI 2020 program. CAP acknowledges the funding received from European Union’s Horizon Europe–Marie Skłodowska-Curie 2021 program through the Postdoctoral Fellowship with Reference 101065902 (ORION). This work is supported by the ANR projects OPLA (ANR-20-CE30-0014) and FEN-NEC (ANR-23-CE30-0042).

-
- [1] T. Schmiedl and U. Seifert, Optimal Finite-Time Processes In Stochastic Thermodynamics, *Physical Review Letters* **98**, 108301 (2007).
- [2] A. Gomez-Marin, T. Schmiedl, and U. Seifert, Optimal protocols for minimal work processes in underdamped stochastic thermodynamics, *The Journal of Chemical Physics* **129**, 024114 (2008).
- [3] E. Aurell, C. Mej a-Monasterio, and P. Muratore-Ginanneschi, Optimal Protocols and Optimal Transport in Stochastic Thermodynamics, *Physical Review Letters* **106**, 250601 (2011).
- [4] E. Aurell, K. Gawedzki, C. Mejia-Monasterio, R. Mohayae, and P. Muratore-Ginanneschi, Refined Second Law of Thermodynamics for Fast Random Processes, *Journal of Statistical Physics* **147**, 487 (2012).
- [5] P. Muratore-Ginanneschi, On extremals of the entropy production by ‘Langevin–Kramers’ dynamics, *Journal of Statistical Mechanics: Theory and Experiment* **2014**, P05013 (2014).
- [6] Y. Zhang, Work needed to drive a thermodynamic system between two distributions, *EPL (Europhysics Letters)* **128**, 30002 (2020).
- [7] S. A. Loos, S. Monter, F. Ginot, and C. Bechinger, Universal symmetry of optimal control at the microscale, *Physical Review X* **14**, 021032 (2024).
- [8] G. C. Hegerfeldt, Driving at the Quantum Speed Limit: Optimal Control of a Two-Level System, *Physical Review Letters* **111**, 260501 (2013).
- [9] G. C. Hegerfeldt, High-speed driving of a two-level system, *Physical Review A* **90**, 032110 (2014).
- [10] C. A. Plata, D. Gu ery-Odelin, E. Trizac, and A. Prados, Finite-time adiabatic processes: Derivation and speed limit, *Physical Review E* **101**, 032129 (2020).
- [11] A. Prados, Optimizing the relaxation route with optimal control, *Physical Review Research* **3**, 023128 (2021).
- [12] A. Patr on, A. Prados, and C. A. Plata, Thermal brachistochrone for harmonically confined Brownian particles, *The European Physical Journal Plus* **137**, 1011 (2022).
- [13] D. A. Sivak and G. E. Crooks, Thermodynamic Metrics and Optimal Paths, *Physical Review Letters* **108**, 190602 (2012).
- [14] S. Ito, Stochastic Thermodynamic Interpretation of Information Geometry, *Physical Review Letters* **121**, 030605 (2018).
- [15] N. Shiraishi, K. Funo, and K. Saito, Speed Limit for Classical Stochastic Processes, *Physical Review Letters* **121**,

- 070601 (2018).
- [16] S. Ito and A. Dechant, Stochastic time-evolution, information geometry and the Cramer-Rao Bound, *Physical Review X* **10**, 021056 (2020).
- [17] T. Van Vu and Y. Hasegawa, Thermodynamic uncertainty relations under arbitrary control protocols, *Physical Review Research* **2**, 013060 (2020).
- [18] Negative values of the stiffness are difficult to implement in the lab, although they have been realized employing feedback techniques [50].
- [19] L. S. Pontryagin, *Mathematical Theory of Optimal Processes* (CRC Press, 1987).
- [20] D. Guéry-Odelin, C. Jarzynski, C. A. Plata, A. Prados, and E. Trizac, Driving rapidly while remaining in control: classical shortcuts from Hamiltonian to stochastic dynamics, *Reports on Progress in Physics* **86**, 035902 (2023).
- [21] S. Blaber and D. A. Sivak, Optimal control in stochastic thermodynamics, *Journal of Physics Communications* **7**, 033001 (2023).
- [22] I. A. Martínez, A. Petrosyan, D. Guéry-Odelin, E. Trizac, and S. Ciliberto, Engineered swift equilibration of a Brownian particle, *Nature Physics* **12**, 843 (2016).
- [23] G. Li, H. T. Quan, and Z. C. Tu, Shortcuts to isothermality and nonequilibrium work relations, *Physical Review E* **96**, 012144 (2017).
- [24] C. A. Plata, D. Guéry-Odelin, E. Trizac, and A. Prados, Optimal work in a harmonic trap with bounded stiffness, *Physical Review E* **99**, 012140 (2019).
- [25] C. A. Plata, A. Prados, E. Trizac, and D. Guéry-Odelin, Taming the Time Evolution in Overdamped Systems: Shortcuts Elaborated from Fast-Forward and Time-Reversed Protocols, *Physical Review Letters* **127**, 190605 (2021).
- [26] S. Ciliberto, Experiments in Stochastic Thermodynamics: Short History and Perspectives, *Physical Review X* **7**, 021051 (2017).
- [27] I. A. Martínez, E. Roldán, L. Dinis, and R. A. Rica, Colloidal heat engines: a review, *Soft Matter* **13**, 22 (2017).
- [28] D. Guéry-Odelin, A. Ruschhaupt, A. Kiely, E. Torrontegui, S. Martínez-Garaot, and J. G. Muga, Shortcuts to adiabaticity: Concepts, methods, and applications, *Reviews of Modern Physics* **91**, 045001 (2019).
- [29] A. Le Cunuder, I. A. Martínez, A. Petrosyan, D. Guéry-Odelin, E. Trizac, and S. Ciliberto, Fast equilibrium switch of a micro mechanical oscillator, *Applied Physics Letters* **109**, 113502 (2016).
- [30] L. Rondin, J. Gieseler, F. Ricci, R. Quidant, C. Delgado, and L. Novotny, Direct measurement of Kramers turnover with a levitated nanoparticle, *Nature Nanotechnology* **12**, 1130 (2017).
- [31] M. Rademacher, M. Konopik, M. Debiossac, D. Grass, E. Lutz, and N. Kiesel, Nonequilibrium Control of Thermal and Mechanical Changes in a Levitated System, *Physical Review Letters* **128**, 070601 (2022).
- [32] S. Dago and L. Bellon, Dynamics of Information Erasure and Extension of Landauer's Bound to Fast Processes, *Physical Review Letters* **128**, 070604 (2022).
- [33] D. Raynal, T. De Guillebon, D. Guéry-Odelin, E. Trizac, J.-S. Lauret, and L. Rondin, Shortcuts to Equilibrium with a Levitated Particle in the Underdamped Regime, *Physical Review Letters* **131**, 087101 (2023).
- [34] M. Chupeau, S. Ciliberto, D. Guéry-Odelin, and E. Trizac, Engineered swift equilibration for Brownian objects: from underdamped to overdamped dynamics, *New Journal of Physics* **20**, 075003 (2018).
- [35] G. Li, J.-F. Chen, C. Sun, and H. Dong, Geodesic Path for the Minimal Energy Cost in Shortcuts to Isothermality, *Physical Review Letters* **128**, 230603 (2022).
- [36] P. Muratore-Ginanneschi and K. Schwieger, How nanomechanical systems can minimize dissipation, *Phys. Rev. E* **90**, 060102 (2014).
- [37] C. A. Plata, D. Guéry-Odelin, E. Trizac, and A. Prados, Building an irreversible Carnot-like heat engine with an overdamped harmonic oscillator, *Journal of Statistical Mechanics: Theory and Experiment* **2020**, 093207 (2020).
- [38] J. Sanders, M. Baldovin, and P. Muratore-Ginanneschi, Optimal control of underdamped systems: An analytic approach (2024), arXiv:2403.00679 [cond-mat.stat-mech].
- [39] J. Sanders, M. Baldovin, and P. Muratore-Ginanneschi, Minimal-work protocols for inertial particles in non-harmonic traps (2024), arXiv:2407.15678 [cond-mat.stat-mech].
- [40] S. Shankar, V. Raju, and L. Mahadevan, Optimal transport and control of active drops, *Proceedings of the National Academy of Sciences* **119**, 10.1073/pnas.2121985119 (2022).
- [41] H. Massana-Cid, C. Maggi, G. Frangipane, and R. Di Leonardo, Rectification and confinement of photokinetic bacteria in an optical feedback loop, *Nature Communications* **13**, 2740 (2022).
- [42] M. Baldovin, D. Guéry-Odelin, and E. Trizac, Control of active brownian particles: An exact solution, *Phys. Rev. Lett.* **131**, 118302 (2023).
- [43] L. K. Davis, K. Proesmans, and E. Fodor, Active matter under control: Insights from response theory, *Phys. Rev. X* **14**, 011012 (2024).
- [44] D. Liberzon, *Calculus of Variations and Optimal Control Theory: A Concise Introduction* (Princeton University Press, 2012).
- [45] C. Gardiner, *Stochastic Methods: A Handbook for the Natural and Social Sciences*, Springer Series in Synergetics (Springer Berlin Heidelberg, 2009).
- [46] X. Chen, A. Ruschhaupt, S. Schmidt, A. del Campo, D. Guéry-Odelin, and J. G. Muga, Fast Optimal Frictionless Atom Cooling in Harmonic Traps: Shortcut to Adiabaticity, *Physical Review Letters* **104**, 063002 (2010).
- [47] X.-J. Lu, X. Chen, J. Alonso, and J. G. Muga, Fast transitionless expansions of Gaussian anharmonic traps for cold atoms: Bang-singular-bang control, *Physical Review A* **89**, 023627 (2014).
- [48] Y. Ding, T.-Y. Huang, K. Paul, M. Hao, and X. Chen, Smooth bang-bang shortcuts to adiabaticity for atomic transport in a moving harmonic trap, *Physical Review A* **101**, 063410 (2020).
- [49] N. Ruiz-Pino and A. Prados, Optimal Control of Uniformly Heated Granular Fluids in Linear Response, *Entropy* **24**, 131 (2022).
- [50] J. A. C. Albay, P.-Y. Lai, and Y. Jun, Realization of finite-rate isothermal compression and expansion using optical feedback trap, *Applied Physics Letters* **116**, 103706 (2020).

Supplemental Information for “Optimal control of levitated nanoparticles through finite-stiffness confinement”

Marco Baldovin,^{1,2,*} Ines Ben Yedder,³ Carlos A. Plata,⁴ Damien Raynal,^{3,5} Loïc Rondin,³ Emmanuel Trizac,^{2,6} and Antonio Prados⁴

¹*Institute for Complex Systems, CNR, Rome, I-00185 Italy*

²*Université Paris-Saclay, CNRS, LPTMS, Orsay, F-91405 France*

³*Université Paris-Saclay, ENS Paris-Saclay, CentraleSupélec, CNRS, LuMIN, Orsay, F-91405 France*

⁴*Física Teórica, Universidad de Sevilla, Apartado de Correos 1065, Sevilla, E-41080 Spain*

⁵*Present address: Centre of Light for Life (CLL) and Institute for Photonics and Advanced Sensing (IPAS), The University of Adelaide, Adelaide, 5005, SA, Australia*

⁶*École Normale Supérieure de Lyon, Lyon, F-69342 France*

(Dated: August 2, 2024)

I. DERIVATION OF THE COST FUNCTION

We want to compute an explicit expression for

$$\langle W \rangle = \int_0^{t_f} dt P(t) = \int_0^{t_f} dt \int_{-\infty}^{\infty} dx \int_{-\infty}^{\infty} dv p(x, v, t) \partial_t U(x, t), \quad (\text{S1})$$

where $U(x, t)$ is the time-dependent external potential, and we denoted by $P(t)$ the (average) instantaneous power. Even if we are only interested in the particular case

$$U(x, t) = \frac{\kappa(t)}{2} x^2,$$

it is useful to consider the problem in its full generality. See also [1] for an alternative derivation.

An integration by parts leads to

$$P(t) = \partial_t \langle U \rangle - \int_{-\infty}^{\infty} dx \int_{-\infty}^{\infty} dv U(x, t) \partial_t p(x, v, t), \quad (\text{S2})$$

hence by recalling the Klein-Kramers equation

$$\partial_t p(x, v, t) = -\partial_x [vp(x, v, t)] + \frac{1}{m} \partial_v \left(\partial_x U(x, t) p(x, v, t) + \gamma v p(x, v, t) + \frac{\gamma k_B T}{m} \partial_v p(x, v, t) \right), \quad (\text{S3})$$

we get

$$P(t) = \partial_t \langle U \rangle - \langle v \partial_x U(x, t) \rangle. \quad (\text{S4})$$

We now multiply both sides of (S3) by $mv^2/2$ and integrate in x and v , obtaining

$$\partial_t \left\langle \frac{mv^2}{2} \right\rangle = -\langle v \partial_x U(x, t) \rangle - \gamma \langle v^2 \rangle + \frac{\gamma}{m} k_B T.$$

Once inserted into (S4) the above relation yields

$$\begin{aligned} P(t) &= \partial_t \langle U \rangle + \partial_t \left\langle \frac{mv^2}{2} \right\rangle + \gamma \langle v^2 \rangle - \frac{\gamma}{m} k_B T \\ &= \partial_t \langle E \rangle + \gamma \langle v^2 \rangle - \frac{\gamma}{m} k_B T, \end{aligned} \quad (\text{S5})$$

* marco.baldovin@cnr.it

where $\langle E \rangle$ is the average mechanical energy of the particle. From (S1), one thus gets

$$\langle W \rangle = \langle E(t_f) \rangle - \langle E(0) \rangle + \gamma \int_0^{t_f} dt \langle v^2 \rangle - \frac{\gamma}{m} k_B T t_f. \quad (\text{S6})$$

The minimization of the work, once the boundary conditions are fixed, is therefore equivalent to the minimization of the cost function

$$C = \gamma \int_0^{t_f} dt \langle v^2 \rangle - \frac{\gamma}{m} k_B T t_f. \quad (\text{S7})$$

Reasoning in the same way, we can as well relate the average instantaneous power to the average free energy

$$\langle F \rangle = \langle E \rangle - TS$$

where the entropy S is defined as

$$S = -k_B \int_{-\infty}^{\infty} dx \int_{-\infty}^{\infty} dv p(x, v, t) \ln p(x, v, t). \quad (\text{S8})$$

By repeated use of (S3) and integration by parts, one finds

$$\partial_t S = \frac{k_B^2 \gamma T}{m^2} \int_{-\infty}^{\infty} dx \int_{-\infty}^{\infty} dv p(x, v, t) (\partial_v \ln p(x, v, t))^2 - \frac{k_B \gamma}{m}. \quad (\text{S9})$$

Equation (S6) can thus be recast as

$$\begin{aligned} \langle W \rangle &= \langle F(t_f) \rangle - \langle F(0) \rangle + \gamma \int_0^{t_f} dt \int_{-\infty}^{\infty} dx \int_{-\infty}^{\infty} dv \left(v + \frac{k_B T}{m} \partial_v \ln p(x, v, t) \right)^2 p(x, v, t) \\ &= \langle F(t_f) \rangle - \langle F(0) \rangle + \langle W_{\text{irr}} \rangle. \end{aligned} \quad (\text{S10})$$

Consistently with the second principle, the irreversible part $\langle W_{\text{irr}} \rangle$ of the average work is always non-negative, and it vanishes only at equilibrium. The minimal work is therefore attained along a quasi-static processes, where the instantaneous distribution is always of the Maxwell-Boltzmann type.

II. OPTIMAL WORK FOR t_f CLOSE TO t_{th}

In the main text we argue that, if the total time t_f is fairly larger than the threshold t_{th} , a minimal-work solution can be found in the form of a 3-stage protocol. The first and the last steps are performed at constant $k = k_{\pm}$ (the sign depends on the case), while the intermediate stage is given by the solution $k_0(s)$ of the Euler-Lagrange equations. In this section, we show some explicit numerical examples to gain insight into the case of t_f close to t_{th} .

In Fig. 1 we show the explicit 3-stage solution for different values of the total time t_f and of the upper bound k_+ , with $k_- = 0$. As expected, when t_f is long enough, the solution built in this way is admissible, meaning that $k_0(s)$ never exceeds the interval $[k_-, k_+]$. However, as t_f approaches t_{th} , the optimal solution tends to span a wider range of values for the stiffness, eventually exceeding the bounds on k —see panels (f), (j) and (k) of Fig. 1.

Since $t_f > t_{\text{th}}$, we know that completing a transition between the prescribed initial and final states must be possible. We also know that, among the many possible solutions, the one requiring minimal average work must satisfy Pontryagin's maximum principle. We may therefore search for 4-stage protocols of the form

$$k(s) = \begin{cases} k_{\pm}, & 0 \leq t < t_1, \\ k_0(s), & t_1 \leq t < t^*, \\ k_{\mp}, & t^* \leq t < t_2, \\ k_{\pm}, & t_2 \leq t < t_f, \end{cases} \quad \text{or} \quad k(s) = \begin{cases} k_{\pm}, & 0 \leq t < t_1, \\ k_{\mp}, & t_1 \leq t < t^*, \\ k_0(s), & t^* \leq t < t_2, \\ k_{\pm}, & t_2 \leq t < t_f, \end{cases} \quad (\text{S11})$$

where $s = \gamma t/m$, with the initial sign depending on the boundary conditions. Both forms are in principle allowed by Pontryagin's condition: one can discriminate between the two on the basis of a visual inspection of the unbounded solution, and invoking a continuity argument. The time t^* needs to be found through a numerical minimization of the cost function.

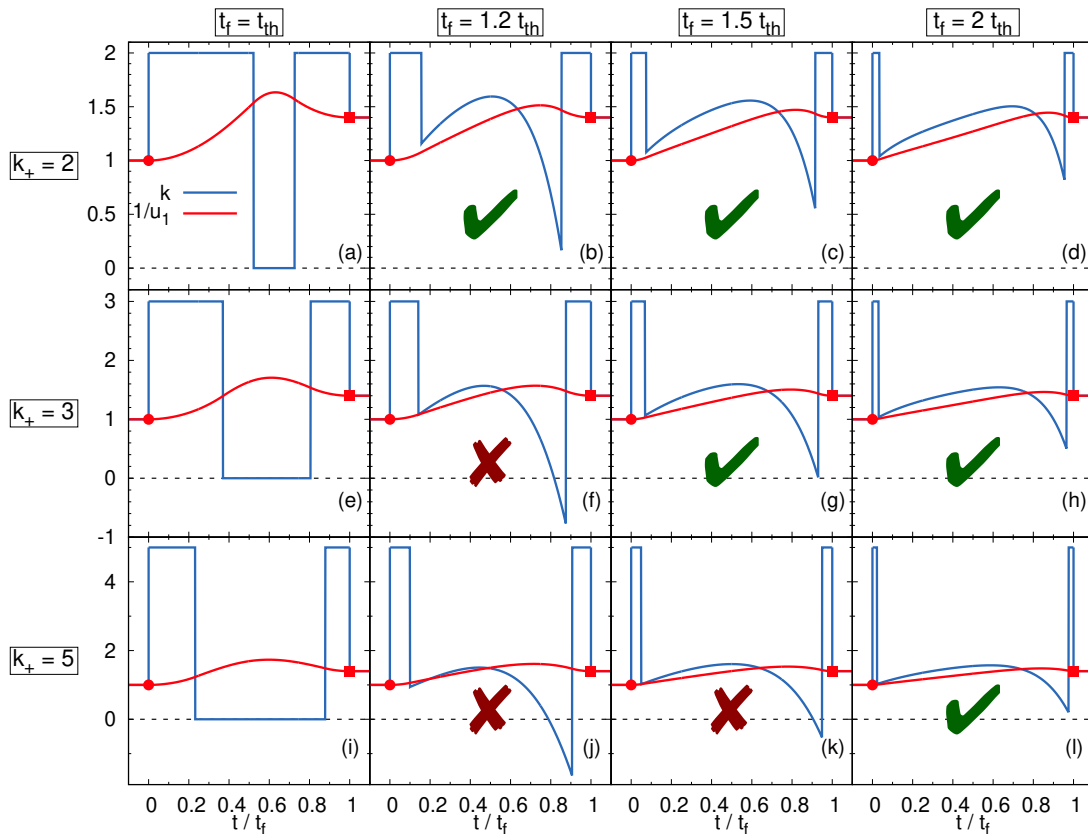


FIG. 1. Minimal work protocols. In each panel the optimal protocol k (blue) and the inverse of the position variance $1/u_1$ (red) are shown. The leftmost column [panels (a), (e) and (i)] shows the 3-step minimal time protocol, which takes place by definition in a rescaled time t_{th} . We expect this process to be the only possible one for $t_f = t_{th}$, given the bounds $k_- \leq k \leq k_+$, and therefore to be also the minimal-work process for that time horizon. The second, third and fourth column show the (tentative) minimal-work 3-stage protocols for $t_f = 1.2t_{th}$, $t_f = 1.5t_{th}$ and $t_f = 2t_{th}$. Different rows correspond to different values of k_+ , for fixed $k_- = 0$. We notice that the prescribed recipe to build the minimal-time protocol fails in the cases of panels (f), (j) and (k), as the protocol found by solving the differential system for $t_1 < t < t_2$ exceeds the bounds. Here $k_i = 1$, $k_f = 1.4$.

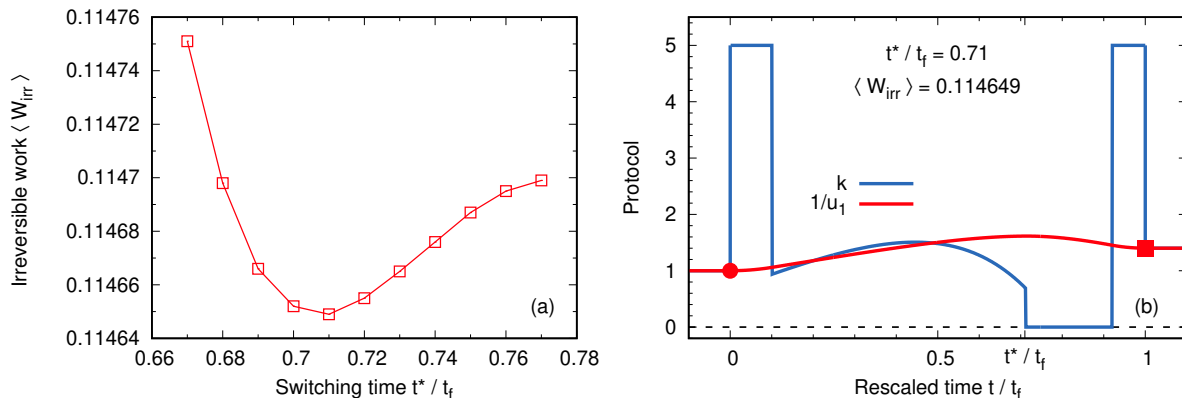


FIG. 2. Selection of the optimal 4-stage protocol. Panel (a) shows the value of the average irreversible work, in dimensionless units, as a function of the switching time t^* appearing in (S11). By inspection of this curve, one can select empirically the value corresponding to the minimal work (here $t^* \simeq 0.71t_f$). In panel (b) the corresponding protocol is shown, with the same color code as in Fig. 1. The parameters are the same of panel (j) of Fig. 1.

Here we consider the explicit example of panel (j) of Fig. 1. Since k_0 , in the 3-stage solution, gets lower than k_- just before the switching time t_2 , we expect the first of the protocols (S11) to be the correct one, by continuity. We

thus compute the work obtained by such protocols for different values of t^* : the results of this analysis are shown in Fig. 2(a). We observe that the irreversible work attains a minimum, which corresponds therefore to the optimal protocol (at least, among the 4-stage protocols that we are considering). Its explicit form is shown in Fig. 2(b).

A similar reasoning can be applied to every non-admissible plot in Fig 1. We obtain in this way the “amended” Fig 3. For values of t_f even closer to t_{th} , more complex protocols may arise. The study of these quite specific situations is out of the the scope of the present paper.

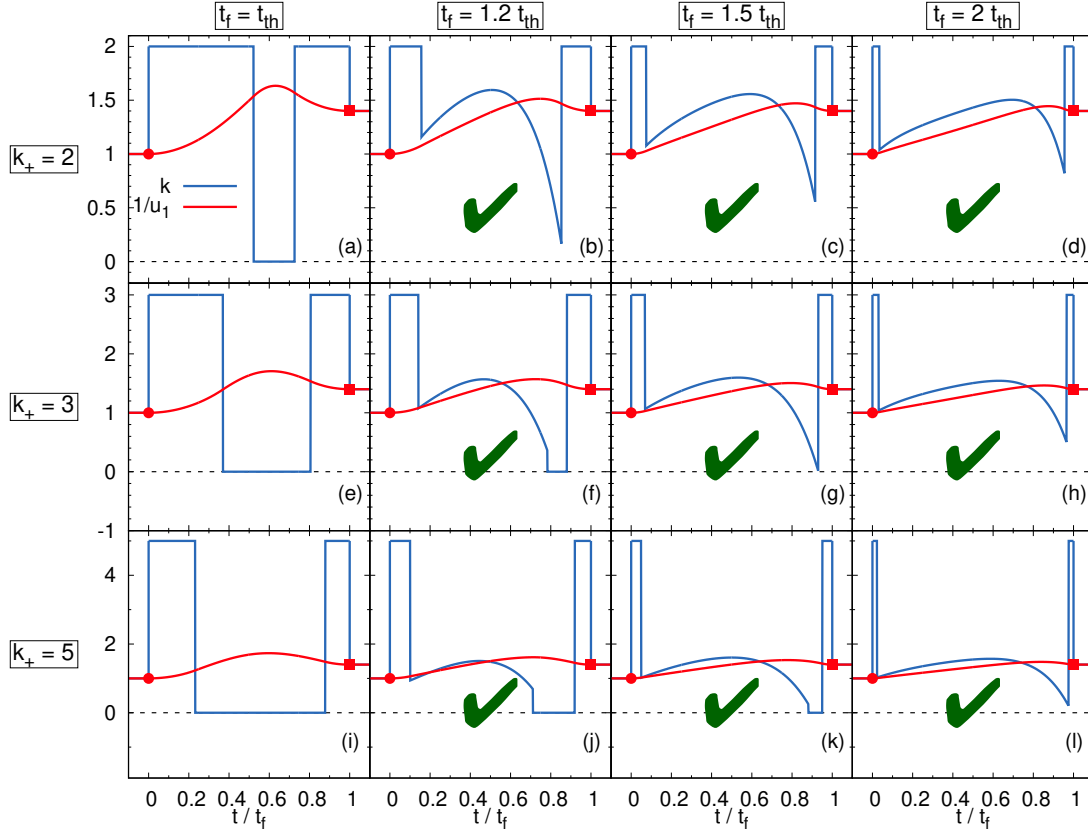


FIG. 3. Same as in Fig. 1, where panels (f), (j) and (k) have been replaced by 4-stage protocols obtained as shown in Fig. 2.

[1] P. Muratore-Ginanneschi, On extremals of the entropy production by ‘Langevin–Kramers’ dynamics, *Journal of Statistical Mechanics: Theory and Experiment* **2014**, P05013 (2014).